

BOPC1 Enantiomers Preparation and HuR Interaction Study. From Molecular Modeling to a Curious DEEP-STD NMR Application

Serena Della Volpe, Roberta Listro, Michela Parafioriti, Marcello Di Giacomo, Daniela Rossi, Francesca Alessandra Ambrosio, Giosuè Costa,* Stefano Alcaro, Francesco Ortuso, Anna K. H. Hirsch, Francesca Vasile,* and Simona Collina*

Cite This: *ACS Med. Chem. Lett.* 2020, 11, 883–888

Read Online

ACCESS |

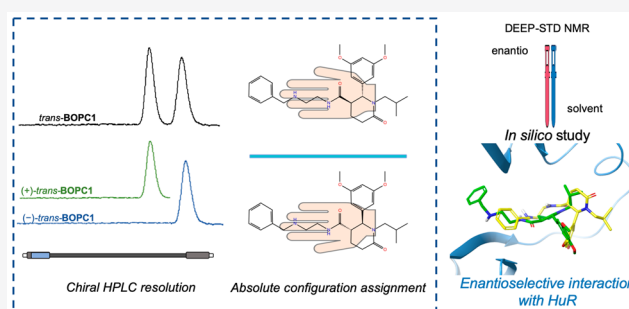
Metrics & More

Article Recommendations

Supporting Information

ABSTRACT: The Hu family of RNA-binding proteins plays a crucial role in post-transcriptional processes; indeed, Hu–RNA complexes are involved in various dysfunctions (i.e., inflammation, neurodegeneration, and cancer) and have been recently proposed as promising therapeutic targets. Intrigued by this concept, our research efforts aim at identifying small molecules able to modulate HuR–RNA interactions, with a focus on subtype HuR, upregulated and dysregulated in several cancers. By applying structure-based design, we had already identified racemic *trans*-BOPC1 as promising HuR binder. In this Letter, we accomplished the enantio-resolution, the assignment of the absolute configuration, and the recognition study with HuR of enantiomerically pure *trans*-BOPC1. For the first time, we apply DEEP (differential epitope mapping)-STD NMR to study the interaction of BOPC1 with HuR and compare its enantiomers, gaining information on ligand orientation and amino acids involved in the interaction, and thus increasing focus on the *in silico* binding site model.

KEYWORDS: RNA-binding protein, HuR–RNA complexes, molecular modeling, chiral HPLC, DEEP-STD NMR



RNA-binding proteins (RBPs) are considered relevant targets to modulate gene expression and therefore to face several pathologies such as neurodegeneration and cancer.^{1–8} While most approaches focus on RNA interference-based oligonucleotides targeting different RNA-binding domains (RBDs),^{9–13} a more recent strategy involves the identification of small molecules able to modulate ribonucleoprotein (RNP) complexes. This strategy is intrinsically challenging, because RBPs generally lack a defined small-molecule binding site. In this context, in 2018, H3B-8800,¹⁴ a small molecule acting as an inhibitor of SF3b, a protein with critical functions in pre-mRNA splicing, reached the first stage of clinical phase for selected types of leukemia. This is the first rationally designed small molecule able to target RBPs to reach the clinic, and therefore, it represents a milestone in the story of RBP modulation, confirming that this strategy represents a way to develop new effective therapeutic agents.

Within our medicinal chemistry research group, we have been working in this field for several years, particularly studying the Hu protein family, a RBP class with a pivotal role in the stabilization of various RNAs.^{2,15–18} Among Hu proteins, HuR is the most studied, as it is an intriguing target for discovering new anticancer drugs.^{19,20} Nevertheless, to date little is known about the features of the HuR–small molecule interaction, even for proven interferers.^{21–23} In this context, to

supply the lack of structural data and with the aim of discovering new HuR ligands able to modulate HuR–RNA binding, we exploit highly informative NMR methodologies combined with *in silico* studies.^{24–28} Briefly, according to a structure-based approach, we have focused on a pocket-like region of HuR formed by the RNP1 and RNP2 portions of RRM1 and 2 (RNA-recognition motif-type domain). Within the HuR RRM1/2–RNA^{c-fos} cocrystal (PDB 4ED5),²⁹ this region corresponds to the binding site of RNA–uridine residues 8 and 9 (U8–U9); thus, their position and key interactions represented the starting point (anchor) to our design of new HuR ligands. New compounds characterized by different cores were designed, synthesized, and subjected to a combined STD (saturation transfer difference) NMR and *in silico* investigation of their interactions with HuR.²⁸

N-(2-(Benzylamino)ethyl)-2-(3,5-dimethoxyphenyl)-1-isobutyl-6-oxopiperidine-3-carboxamide, from now on BOPC1 (see Scheme 1), was effective in binding the target protein

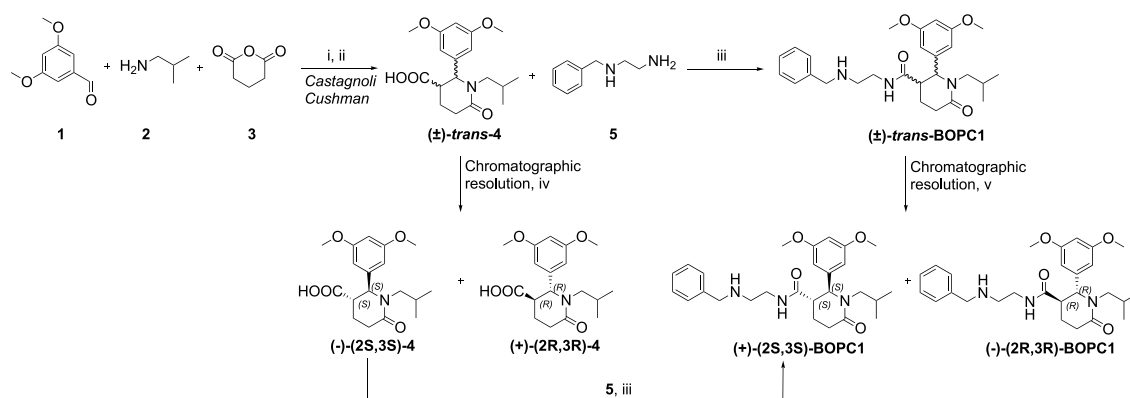
Special Issue: In Memory of Maurizio Botta: His Vision of Medicinal Chemistry

Received: December 28, 2019

Accepted: January 28, 2020

Published: January 28, 2020



Scheme 1. Synthetic Pathway of BOPC1^a

^a(i) 1,2, toluene, MS 4 Å, rt, 4 h; (ii) 3, *p*-xylene, reflux, 12 h, yield 60%; (iii) TBTU, DIPEA, THF, rt, 12 h, yield 71%; (iv) Chiralpak IA column, IPA:DEA:TFA 100:0.1:0.3 (v/v/v), flow rate 2 mL/min, injection volume 1 mL, concentration 10 mg/mL; (v) Chiralpak IC column, *n*-hexane:IPA:DEA 75:25:0.1 (v/v/v), flow rate 2 mL/min, injection volume 1 mL, concentration 10 mg/mL.

HuR. BOPC1 is characterized by the presence of two chiral centers, and in our preliminary experiments, it was tested as the *trans*-racemate. Since it is well recognized that enantiomers of chiral bioactive molecules may have a different interaction with the target, prior to the design of new derivatives, it is mandatory to study *trans*-BOPC1 in its enantiomerically pure forms. In this Letter, we accomplished the enantio-resolution of racemic *trans*-BOPC1, the assignment of the absolute configuration of the separated enantiomers, and their recognition study with HuR.

As a first step, we investigated the binding mode of the two *trans*-configured enantiomers in the previously considered HuR binding pocket, through molecular modeling simulations. The results of the *in silico* analysis, performed on the crystal structure of the HuR RRM1/2 domains, according to the computational approach recently we had published,^{27,28} clearly suggested a stereoselective binding mode (see Figure 1). In fact, though the two enantiomers bind to similar regions of the HuR binding pocket, they do it in a different way, and in order to evaluate the ligand binding free energy (ΔG_{bind}) for BOPC1 enantiomers, the MM-GBSA calculations were performed [(2*R*,3*R*)-BOPC1MMGBSA value -41.27 kcal/mol and (2*S*,3*S*)-BOPC1MMGBSA value -53.37 kcal/mol].

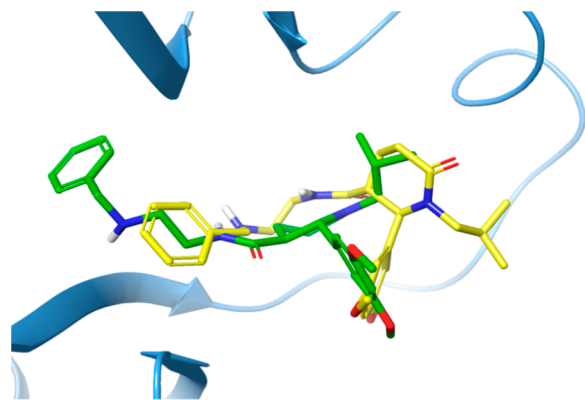


Figure 1. 3D representation of (2*R*,3*R*)- and (2*S*,3*S*)-BOPC1 predicted binding modes overlapped in the HuR binding pocket. The protein is shown as light-blue cartoon, and the (2*S*,3*S*)-BOPC1 and the (2*R*,3*R*)-BOPC1 enantiomers are represented as green and yellow sticks, respectively.

Particularly, docking analysis showed that the aromatic rings of both BOPC1 enantiomers may establish different interactions with HuR.

Prompted by these results, we prepared (2*R*,3*R*)- and (2*S*,3*S*)-BOPC1 and investigated their interaction with HuR.

The synthetic strategy adopted for preparing BOPC1 is outlined in Scheme 1. The intermediate *trans*-2-(3,5-dimethoxyphenyl)-1-isobutyl-6-oxopiperidine-3-carboxylic acid was obtained as a racemate, by a Castagnoli–Cushman reaction, under the experimental conditions we had already described, with slight modifications. The subsequent amidation reaction provided racemic *trans*-BOPC1 (Scheme 1).²⁸

To obtain enantiomerically pure BOPC1 in sufficient amounts for the subsequent studies, we selected chiral high-performance liquid chromatography (HPLC), an effective approach for the resolution of chiral compounds on both analytical and preparative scale.^{30–34} Upon screening various chiral stationary phases (CSPs) and eluents, we obtained a baseline HPLC separation of the two *trans*-BOPC1 enantiomers using the immobilized derivatized-cellulose Chiralcel IC as CSP eluting with *n*-hexane/isopropyl alcohol/DEA 75/25/0.1 (v/v/v). The good enantioselectivity and efficiency of the methodology allowed for an effective scale-up at the semipreparative level. By using a semi-preparative IC column, we resolved 10 mg of sample for each HPLC run, finally isolating about 20 mg of enantiomers with an enantiomeric excess >98%.

To assign the absolute configuration to *trans*-BOPC1 enantiomers, we followed a multistep strategy, consisting in (i) chiral resolution of the key intermediate 4, (ii) assignment of the absolute configuration to (+)-*trans*-4 and (–)-*trans*-4, and (iii) synthesis of enantiomeric BOPC1, starting from enantiomerically pure 4.

Once again, the chiral resolution of the key intermediate (\pm) -*trans*-4 was performed via enantioselective HPLC. In this case a good resolution was obtained using the immobilized amylose chiral Chiralpak IA column under reverse phase elution conditions, eluting with isopropyl alcohol as mobile phase. Both enantiomers of *trans*-4 were obtained in a 50-mg scale, a suitable amount for further studies and with an enantiomeric excess >90%.

As a first step of the empirical approach to assign the absolute configuration of enantiomerically pure *trans*-4, we

used the enantiomers of the structurally related compound *trans*-6 (Figure 2) as a reference. Briefly, we compared both

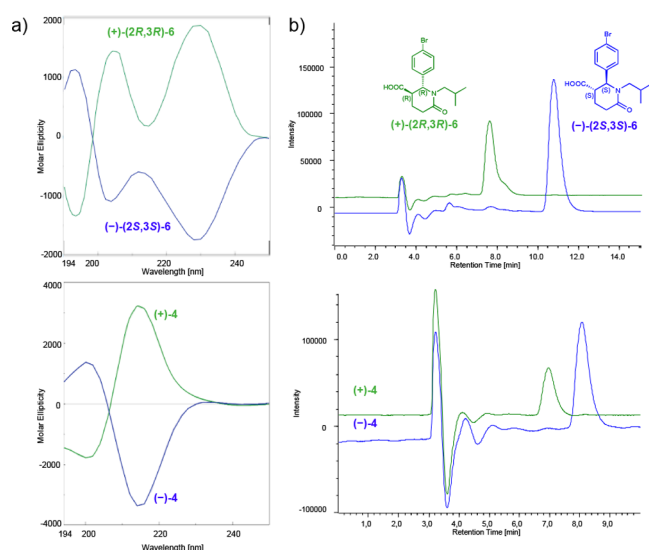


Figure 2. (a) ECD traces in acetonitrile and (b) chromatographic profiles at 220 nm (Chiralpak IA, mobile phase *n*-hexane:IPA:DEA:TFA 75:25:0.1:0.3, flow rate 0.5 mL/min) of (+)-(2*R*,3*R*)-6 and (-)-(2*S*,3*S*)-6 (top), and (+)-*trans*-4 and (-)-*trans*-4 (bottom). For (+) enantiomers the traces are reported in green, for (-) in blue.

the electronic circular dichroism (ECD) spectra and the elution order, under the same chiral chromatographic conditions, of (+)-*trans*-4 and (-)-*trans*-4 with the structurally related (+)-(2*R*,3*R*)-6 and (-)-(2*S*,3*S*)-6, for which we have already assigned the absolute configuration by X-ray crystallographic analysis.³⁵ The ECD spectra of *trans*-4 and the reference compound *trans*-6, recorded in acetonitrile, are shown in Figure 2a. As expected, the enantiomeric forms of *trans*-4 exhibited specular patterns. The findings of the ECD measurements allowed us to define a parallelism between absolute configuration and CD band signs. Briefly, comparable Cotton effects (CEs) for (+)-4 and (+)-(2*R*,3*R*)-6 compounds are evident in two ranges of wavelengths: negative CEs between 190 and 200 nm and positive CEs between 210 and 230 nm attributable to 1*La* and 1*Lb* electronic transitions of benzene. The sign of the CEs of 1*La* is consistently opposite that at the longer wavelength (1*Lb*). For compound (2*R*,3*R*)-6 a twisting of the 1*Lb* band is observed, in accordance with related literature.³⁶ Based on these considerations, the (2*R*,3*R*) absolute configuration of (+)-6 may also be proposed for the first eluted (+)-*trans*-4. Naturally, a reversed sign of the ellipticity is expected from the second eluted (2*S*,3*S*)-enantiomer. The analysis performed on the Chiralpak IA column under the same elution conditions (*n*-hexane:IPA:DEA:TFA 75:25:0.1:0.3) confirmed the same elution order for the enantiomers of both compounds (see Figure 2b).

Once it was determined the absolute configuration of the two enantiomers of the key intermediate was *trans*-4, the stereochemical assignment was extended to the stereoisomers of *trans*-BOPC1 by a chemical correlation method (see Scheme 1). The reaction of connection between the acid intermediate and amine 5 is a stereoconservative process. So, the absolute configuration of each single stereoisomer of *trans*-BOPC1 is determined by the stereochemistry of the enantiomerically pure key intermediate used in its synthesis.

The stereochemical course of reactions was monitored by the enantioselective HPLC conditions described above. The absolute configurations of the two stereoisomers of *trans*-BOPC1 were then assigned as follows: first eluted isomer (+)-*trans*-BOPC1 as (2*S*,3*S*), and second eluted isomer (-)-*trans*-BOPC1 (2*R*,3*R*).

Once the absolute configuration of enantiomerically pure *trans*-BOPC1 was defined, for the study of their interaction with HuR, we employed STD NMR, a leading ligand-based NMR technique used to characterize ligand–macromolecule interactions as they occur in solution³⁷ and identify ligand moieties important for binding the target.³⁸ The experiment is based on the NOE effect and exploits the transfer of the magnetization from the macromolecule, selectively irradiated, to the ligand. The regions of the ligand closer to the macromolecule receive the magnetization more efficiently than those which are farther, producing differences in signal intensity; data processing into binding epitope maps can elucidate the structural features of the binding event. In particular, we compared the binding modes of the two enantiomers and elucidated additional binding site information by applying differential epitope mapping (DEEP) by STD NMR. This very recent technique can gain additional data to the simple STD experiment thanks to the application of differential conditions. Namely, it can identify the type of protein residues contacting the ligand through the generation of differential epitope maps and, if the 3D structure of the protein is known, it helps in orienting the ligand in the binding pocket, with a higher precision compared to the single STD experiment.^{39,40} In particular, we exploited the two enantiomers for interaction studies with the target HuR according to a DEEP-STD protocol for both comparison of the two enantiomers and to build a differential solvent epitope map. First of all, STD NMR spectra were recorded for both enantiomers of *trans*-BOPC1 in a 100% D₂O buffer. Absolute and relative STD% for each enantiomer are stated in S2.2 of the Supporting Information, along with a schematic representation of each enantiomer epitope mapping.

Nonetheless, absolute STD values coming from different STD spectra cannot be directly compared, due to possible differences in sample preparation or instrument setting. For this reason, in order to obtain a comparison between the interaction of the two separate enantiomers with HuR, we exploited the DEEP equation reported in S2.1 of the Supporting Information.⁴¹ The experiment of (2*S*,3*S*)-BOPC1 was chosen as *exp1* (since the global saturation is larger than that of (2*R*,3*R*)-BOPC1), and the ratio and average ratio of STD intensities over all protons was calculated affording “enantio DEEP-STD” values for each proton. The raw and processed data and Δ STD factors are shown in S2.3 of the Supporting Information and represented schematically in Figure 3. We recorded positive Δ STD factors for the protons of ring B and its methoxy group, while negative Δ STD factors were observed for protons 3, 9–10, and 16. These differences suggest that the two enantiomers interact with the same protons but different orientation into the binding site. Positive Δ STD factors suggest which moieties are most involved in the interaction of (2*S*,3*S*)-BOPC1 with HuR, while negative Δ STD factors are used for (2*R*,3*R*)-BOPC1 and HuR.

We then performed differential solvent experiments on both enantiomers by studying their interaction with HuR in H₂O:D₂O 90:10 and comparing each experiment with the respective one in D₂O, following the literature procedure

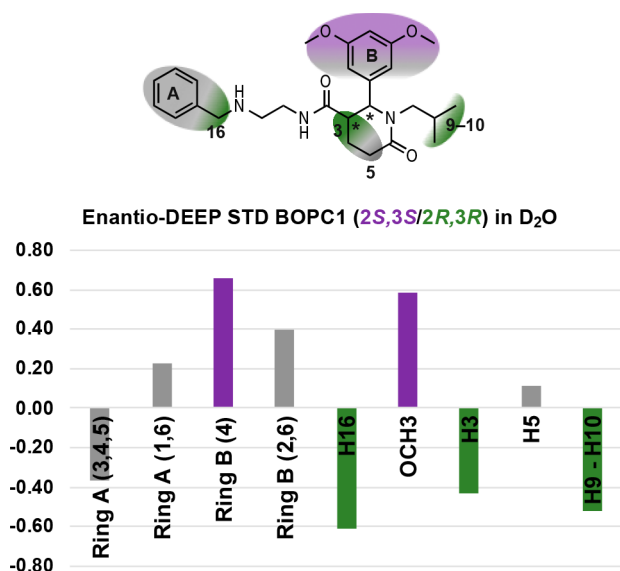


Figure 3. Enantioapplication of the DEEP-STD experiment. The STD spectra of (2*S*,3*S*)-BOPC1 and (2*R*,3*R*)-BOPC1 in D₂O are compared thanks to the equation exploited in the differential approach. Stronger binding components are reported in purple for (2*S*,3*S*)-BOPC1 and dark green for (2*R*,3*R*)-BOPC1. Gray indicates no significant difference in moiety contribution for the two enantiomers tested.

(S2.1).⁴¹ Briefly, DEEP STD negative values (obtained considering D₂O/H₂O ratios) suggest an interaction with exchanging protons of the protein (so, interaction mediated by polar groups). The presence of signals with positive DEEP STD values indicates the involvement in a binding with apolar residues of the protein. The experiment highlighted that for (2*S*,3*S*)-BOPC1, ring A points toward apolar residues, along with protons 5 and 3, while protons 16 and 9–10 are projected toward polar residues. A different interaction was observed for (2*R*,3*R*)-BOPC1: ring A is still interacting with hydrophobic residues, along with 16, while the signals of ring B and its methoxy groups show vicinity to polar residues (all raw and processed data are reported in S2.5 and S2.6 of the Supporting Information).

The data thus obtained were exploited to confirm and refine ligand orientation in the HuR binding pocket. In accordance with experimental data, ring B of (2*R*,3*R*)-BOPC1 (MMGBSA value -41.27 kcal/mol) establishes only an interaction mediated by polar group namely an H-bond with Asn25. Conversely, ring B of the (2*S*,3*S*)-BOPC1 (MMGBSA value -53.37 kcal/mol) can form a stacking interaction with Tyr63 and three H-bonds, with Arg153 and with Asn25; this is mirrored by low DEEP-STD values for this moiety indicating no prevalence of either polar or apolar interactions. Combined DEEP-STD and *in silico* results are shown in Figure 4.

The DEEP-STD protocol, applied in the present Letter to study for the first time the interaction of *trans*-BOPC1 enantiomers with HuR, gains information on the orientation of the compounds in the binding site and elucidates the type of amino acids involved in the binding event. The two binding modes reported in Figure 4 for the two *trans*-BOPC1 enantiomers are the best agreement between best docking poses and DEEP-STD data. Given the precious information originated from the collected spectroscopic and computational data, and with the increased focus on the *in silico* binding site

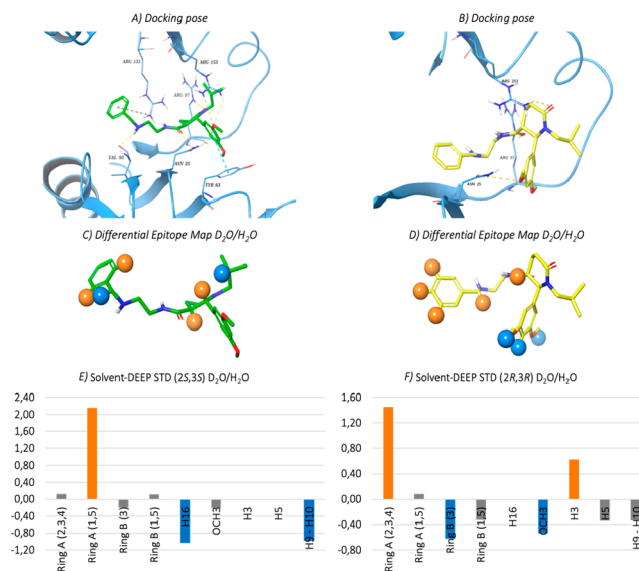


Figure 4. Selected docking pose of the (a) (2*S*,3*S*)-BOPC1 and (b) (2*R*,3*R*)-BOPC1 in the HuR binding pocket. The protein residues involved in crucial contacts with the ligands are reported as light-blue carbon sticks. Hydrogen bonds, *pi*-*pi* stacking and *pi*-cation interactions are reported, respectively, as dashed yellow, light-blue, and green lines. (c,d) Graphic representation of the solvent DEEP-STD experiment on the (2*S*,3*S*)-BOPC1–HuR and (2*R*,3*R*)-BOPC1–HuR complexes. Blue spheres indicate ligand contacts with protein side chains carrying slowly exchanging protons; orange spheres indicate ligand contacts with apolar residues. (e,f) Solvent DEEP-STD histograms of (2*S*,3*S*)-BOPC1–HuR and (2*R*,3*R*)-BOPC1–HuR complexes; blue and orange bars represent contacts with polar and apolar residues, respectively; gray bars indicate no significant difference in type of amino acid contacts for the two solvent conditions tested. For protons 5 and 3 (e) and 16 (f) the DEEP-STD values could not be calculated due to absence of their signal in the H₂O experiment. Nonetheless, the contribution of apolar residues (D₂O experiment) for these protons is still prevalent.

model in hands, we plan to design and synthesize a focused library of novel oxopiperidine-3-carboxamides, to gain complete structure–activity relationships, and to identify leads with improved affinity toward HuR, potentially active against different types of cancer.

■ ASSOCIATED CONTENT

Supporting Information

The Supporting Information is available free of charge at <https://pubs.acs.org/doi/10.1021/acsmchemlett.9b00659>.

Synthesis, enantiomeric resolution by chiral HPLC, and compound characterization. We report all protocols in SI, S1. Interaction studies with HuR STD and DEEP-STD NMR studies were carried out as reported in SI, S2. Molecular modeling molecular dynamics simulations and docking studies were performed as stated in SI, S3. (PDF)

■ AUTHOR INFORMATION

Corresponding Authors

Giosuè Costa – Department of Health Sciences and Net4Science Academic Spin-Off, University “Magna Græcia” of Catanzaro, 88100 Catanzaro, Italy; orcid.org/0000-0003-0947-9479; Email: gcosta@unicz.it

Francesca Vasile – Department of Chemistry, University of Milan, 20133 Milano, Italy; Email: francesca.vasile@unimi.it
Simona Collina – Department of Drug Sciences, Medicinal Chemistry and Technology Section, University of Pavia, 27100 Pavia, Italy; orcid.org/0000-0002-2954-7558; Email: simona.collina@unipv.it

Authors

Serena Della Volpe – Department of Drug Sciences, Medicinal Chemistry and Technology Section, University of Pavia, 27100 Pavia, Italy; Department of Chemistry, University of Milan, 20133 Milano, Italy

Roberta Listro – Department of Drug Sciences, Medicinal Chemistry and Technology Section, University of Pavia, 27100 Pavia, Italy

Michela Parafioriti – Department of Drug Sciences, Medicinal Chemistry and Technology Section, University of Pavia, 27100 Pavia, Italy

Marcello Di Giacomo – Department of Drug Sciences, Medicinal Chemistry and Technology Section, University of Pavia, 27100 Pavia, Italy

Daniela Rossi – Department of Drug Sciences, Medicinal Chemistry and Technology Section, University of Pavia, 27100 Pavia, Italy

Francesca Alessandra Ambrosio – Department of Health Sciences, University “Magna Græcia” of Catanzaro, 88100 Catanzaro, Italy

Stefano Alcaro – Department of Health Sciences and Net4Science Academic Spin-Off, University “Magna Græcia” of Catanzaro, 88100 Catanzaro, Italy

Francesco Ortuso – Department of Health Sciences and Net4Science Academic Spin-Off, University “Magna Græcia” of Catanzaro, 88100 Catanzaro, Italy; orcid.org/0000-0001-6235-8161

Anna K. H. Hirsch – Helmholtz Institute for Pharmaceutical Research Saarland (HIPS)–Helmholtz Centre for Infection Research (HZI), Department of Drug Design and Optimization, 66123 Saarbrücken, Germany; Department of Pharmacy, Saarland University, 66123 Saarbrücken, Germany; orcid.org/0000-0001-8734-4663

Complete contact information is available at:

<https://pubs.acs.org/10.1021/acsmchemlett.9b00659>

Author Contributions

The manuscript was written through contributions of all authors.

Notes

The authors declare no competing financial interest.

ACKNOWLEDGMENTS

FV, SDV, and SC gratefully acknowledge Donatella Potenza for the fruitful scientific discussion and for her contribution to the development of the STD technique and its application to this project; all authors thankfully recognize Alessandro Provenzani and his team for expressing, purifying, and providing native HuR protein utilized for interaction studies. FV acknowledges University of Milano for the grant PSR 2018 (“Piano di Sostegno per la Ricerca” -linea 2). SA and GC acknowledge the PRIN 2017 research project “Novel anticancer agents endowed with multitargeting mechanism of action” (201744BN5T).

ABBREVIATIONS

RBP, RNA-binding protein; RBD, RNA-binding domains; RNP, ribonucleoprotein; RRM, RNA recognition motif-type; STD-NMR, saturation transfer difference-NMR; BOPC1, N-(2-(benzylamino)ethyl)-2-(3,5-dimethoxyphenyl)-1-isobutyl-6-oxopiperidine-3-carboxamide; ECD, electronic circular dichroism; HPLC, high-performance liquid chromatography; CSP, chiral stationary phases; CE, Cotton effects; MMGBSA, molecular mechanism generalized Born surface area

REFERENCES

- (1) Tang, A. Y. RNA Processing-Associated Molecular Mechanisms of Neurodegenerative Diseases. *J. Appl. Genet.* **2016**, *57*, 323–333.
- (2) Kotta-Loizou, I.; Giaginis, C.; Theocharis, S. Clinical Significance of HuR Expression in Human Malignancy. *Med. Oncol.* Published online 13 August **2014**. DOI: [10.1007/s12032-014-0161-y](https://doi.org/10.1007/s12032-014-0161-y).
- (3) Wang, J.; Guo, Y.; Chu, H.; Guan, Y.; Bi, J.; Wang, B. Multiple Functions of the RNA-Binding Protein HuR in Cancer Progression, Treatment Responses and Prognosis. *Int. J. Mol. Sci.* **2013**, *14*, 10015–10041.
- (4) Campos-Melo, D.; Droppelmann, C. A.; Volkening, K.; Strong, M. J. RNA-Binding Proteins as Molecular Links between Cancer and Neurodegeneration. *Biogerontology* **2014**, *15*, 587–610.
- (5) Wurth, L.; Gebauer, F. RNA-Binding Proteins, Multifaceted Translational Regulators in Cancer. *Biochim. Biophys. Acta, Gene Regul. Mech.* **2015**, *1849*, 881–886.
- (6) Dejong, E.; Luy, B.; Marino, J. RNA and RNA-Protein Complexes as Targets for Therapeutic Intervention. *Curr. Top. Med. Chem.* **2002**, *2*, 289–302.
- (7) Talman, V.; Pascale, A.; Jäntti, M.; Amadio, M.; Tuominen, R. K. Protein Kinase C Activation as a Potential Therapeutic Strategy in Alzheimer’s Disease: Is There a Role for Embryonic Lethal Abnormal Vision-like Proteins? *Basic Clin. Pharmacol. Toxicol.* **2016**, *119*, 149–160.
- (8) Talman, V.; Amadio, M.; Osera, C.; Sorvari, S.; Boije Af Gennäs, G.; Yli-Kauhala, J.; Rossi, D.; Govoni, S.; Collina, S.; Ekokoski, E.; et al. The C1 Domain-Targeted Isophthalate Derivative HMI-1b11 Promotes Neurite Outgrowth and GAP-43 Expression through PKC α Activation in SH-SY5Y Cells. *Pharmacol. Res.* **2013**, *73*, 44–54.
- (9) Kim, D. H.; Behlke, M.; Rossi, J. J. Designing and Utilization of siRNAs Targeting RNA Binding Proteins. *Methods Mol. Biol.* **2008**, *488*, 367–381.
- (10) Jacobsen, A.; Wen, J.; Marks, D. S.; Krogh, A. Signatures of RNA Binding Proteins Globally Coupled to Effective MicroRNA Target Sites. *Genome Res.* **2010**, *20*, 1010–1019.
- (11) Guo, X.; Wu, Y.; Hartley, R. S. MicroRNA-125a Represses Cell Growth by Targeting HuR in Breast Cancer. *RNA Biol.* **2009**, *6*, 575–583.
- (12) Makeyev, A. V.; Eastmond, D. L.; Liebhaber, S. A. Targeting a KH-Domain Protein with RNA Decoys. *RNA* **2002**, *8*, 1160–1173.
- (13) Abil, Z.; Zhao, H. Engineering Reprogrammable RNA-Binding Proteins for Study and Manipulation of the Transcriptome. *Mol. Biosyst.* **2015**, *11*, 2658–2665.
- (14) Seiler, M.; Yoshimi, A.; Darman, R.; Chan, B.; Keaney, G.; Thomas, M.; Agrawal, A. A.; Caleb, B.; Csibi, A.; Sean, E.; et al. H3B-8800, an Orally Available Small-Molecule Splicing Modulator, Induces Lethality in Spliceosome-Mutant Cancers. *Nat. Med.* **2018**, *24*, 497–504.
- (15) Hinman, M. N.; Lou, H. Diverse Molecular Functions of Hu Proteins. *Cell. Mol. Life Sci.* **2008**, *65*, 3168–3181.
- (16) Perrone-Bizzozero, N.; Bird, C. W. Role of HuD in Nervous System Function and Pathology. *Front. Biosci., Scholar Ed.* **2013**, *5*, 554–563.
- (17) Antic, D.; Keene, J. D. Embryonic Lethal Abnormal Visual RNA-Binding Proteins Involved in Growth, Differentiation, and

Posttranscriptional Gene Expression. *Am. J. Hum. Genet.* **1997**, *61*, 273–278.

(18) Srikantan, S.; Gorospe, M. HuR Function in Disease. *Front. Biosci., Landmark Ed.* **2012**, *17*, 189–205.

(19) Abdelmohsen, K.; Gorospe, M. Posttranscriptional Regulation of Cancer Traits by HuR. *Wiley Interdiscip. Rev.: RNA* **2010**, *1*, 214–229.

(20) Yuan, Z.; Sanders, A. J.; Ye, L.; Wang, Y.; Jiang, W. G. Prognostic Value of the Human Antigen R (HuR) in Human Breast Cancer: High Level Predicts a Favourable Prognosis. *Anticancer Res.* **2011**, *31*, 303–10.

(21) Nasti, R.; Rossi, D.; Amadio, M.; Pascale, A.; Unver, M. Y.; Hirsch, A. K. H.; Collina, S. Compounds Interfering with Embryonic Lethal Abnormal Vision (ELAV) Protein-RNA Complexes: An Avenue for Discovering New Drugs. *J. Med. Chem.* **2017**, *60*, 8257–8267.

(22) Lal, P.; Cerofolini, L.; D'Agostino, V. G.; Zucal, C.; Fuccio, C.; Bonomo, I.; Dassi, E.; Giuntini, S.; Maio, D. Di; Vishwakarma, V.; et al. Regulation of HuR Structure and Function by Dihydroxanthinone-I. *Nucleic Acids Res.* **2017**, *45*, 9514–9527.

(23) Manzoni, L.; Zucal, C.; Maio, D. Di; D'Agostino, V. G.; Thongon, N.; Bonomo, I.; Lal, P.; Miceli, M.; Baj, V.; Brambilla, M.; et al. Interfering with HuR-RNA Interaction: Design, Synthesis and Biological Characterization of Tanshinone Mimics as Novel, Effective HuR Inhibitors. *J. Med. Chem.* **2018**, *61*, 1483–149.

(24) Rossi, D.; Amadio, M.; Baraglia, A. C.; Azzolina, O.; Ratti, A.; Govoni, S.; Pascale, A.; Collina, S. Discovery of Small Peptides Derived from Embryonic Lethal Abnormal Vision Proteins Structure Showing RNA-Stabilizing Properties. *J. Med. Chem.* **2009**, *52*, 5017–5019.

(25) Amadio, M.; Pascale, A.; Govoni, S.; Laurini, E.; Pricl, S.; Gaggeri, R.; Rossi, D.; Collina, S. Identification of Peptides with ELAV-like mRNA-Stabilizing Effect: An Integrated in Vitro/in Silico Approach. *Chem. Biol. Drug Des.* **2013**, *81*, 707–14.

(26) Vasile, F.; Rossi, D.; Collina, S.; Potenza, D. Diffusion-Ordered Spectroscopy and Saturation Transfer Difference NMR Spectroscopy Studies of Selective Interactions between ELAV Protein Fragments and an mRNA Target. *Eur. J. Org. Chem.* **2014**, *29*, 6399–6404.

(27) Vasile, F.; Della Volpe, S.; Ambrosio, F. A.; Costa, G.; Unver, M. Y.; Zucal, C.; Rossi, D.; Martino, E.; Provenzani, A.; Hirsch, A. K. H.; et al. Exploration of Ligand Binding Modes towards the Identification of Compounds Targeting HuR: A Combined STD-NMR and Molecular Modelling Approach. *Sci. Rep.* Published online September 13, **2018**, DOI: 10.1038/s41598-018-32084-z.

(28) Della Volpe, S.; Nasti, R.; Queirolo, M.; Unver, M. Y.; Jumde, V. K.; Dömling, A.; Vasile, F.; Potenza, D.; Ambrosio, F. A.; Costa, G.; et al. Novel Compounds Targeting the RNA-Binding Protein HuR. Structure-Based Design, Synthesis, and Interaction Studies. *ACS Med. Chem. Lett.* **2019**, *10*, 615–620.

(29) Wang, H.; Zeng, F.; Liu, Q.; Liu, H.; Liu, Z.; Niu, L.; Teng, M.; Li, X. The Structure of the ARE-Binding Domains of Hu Antigen R (HuR) Undergoes Conformational Changes during RNA Binding. *Acta Crystallogr., Sect. D: Biol. Crystallogr.* **2013**, *69*, 373–380.

(30) Rossi, D.; Tarantino, M.; Rossino, G.; Rui, M.; Juza, M.; Collina, S. Approaches for Multi-Gram Scale Isolation of Enantiomers for Drug Discovery. *Expert Opin. Drug Discovery* **2017**, *12*, 1253–1269.

(31) Rossi, D.; Nasti, R.; Collina, S.; Mazzeo, G.; Ghidinelli, S.; Longhi, G.; Memo, M.; Abbate, S. The Role of Chirality in a Set of Key Intermediates of Pharmaceutical Interest, 3-Aryl-Substituted- γ -Butyrolactones, Evidenced by Chiral HPLC Separation and by Chiroptical Spectroscopies. *J. Pharm. Biomed. Anal.* **2017**, *144*, 41–51.

(32) Marra, A.; Rossi, D.; Pignataro, L.; Bigogno, C.; Canta, A.; Oggioni, N.; Malacrida, A.; Corbo, M.; Cavaletti, G.; Peviani, M.; et al. Toward the Identification of Neuroprotective Agents: G-Scale Synthesis, Pharmacokinetic Evaluation and CNS Distribution of (R)-RC-33, a Promising SIGMA1 Receptor Agonist. *Future Med. Chem.* **2016**, *8*, 287–295.

(33) Rossi, D.; Nasti, R.; Marra, A.; Meneghini, S.; Mazzeo, G.; Longhi, G.; Memo, M.; Cosimelli, B.; Greco, G.; Novellino, E.; et al. Enantiomeric 4-Acylamino-6-Alkyloxy-2 Alkylthiopyrimidines As Potential A3Adenosine Receptor Antagonists: HPLC Chiral Resolution and Absolute Configuration Assignment by a Full Set of Chiroptical Spectroscopy. *Chirality* **2016**, *28*, 434–440.

(34) Rossi, D.; Pedrali, A.; Marra, A.; Pignataro, L.; Schepmann, D.; Wünsch, B.; Ye, L.; Leuner, K.; Peviani, M.; Curti, D.; et al. Studies on the Enantiomers of RC-33 as Neuroprotective Agents: Isolation, Configurational Assignment, and Preliminary Biological Profile. *Chirality* **2013**, *25*, 814–822.

(35) Listro, R.; Boiocchi, M.; Della Volpe, S.; Pignataro, L.; Rossi, D.; Rossino, G.; Vasile, F.; Collina, S. Assignment of the absolute configuration of a series of biologically-interesting 2,3-disubstituted- δ -lactams. *Chirality*, unpublished work.

(36) Toda, M.; Inoue, Y.; Mori, T. Circular Dichroisms of Mono- and Dibromo[2.2]Paracyclophanes: A Combined Experimental and Theoretical Study. *ACS Omega* **2018**, *3*, 22–29.

(37) Mayer, M.; Meyer, B. Characterization of Ligand Binding by Saturation Transfer Difference NMR Spectroscopy. *Angew. Chem., Int. Ed.* **1999**, *38*, 1784–1788.

(38) Viegas, A.; Manso, J.; Nobrega, F. L.; Cabrita, E. J. Saturation-Transfer Difference (STD) NMR: A Simple and Fast Method for Ligand Screening and Characterization of Protein Binding. *J. Chem. Educ.* **2011**, *88*, 990–994.

(39) Sattin, S.; Panza, M.; Vasile, F.; Berni, F.; Goti, G.; Tao, J.; Moroni, E.; Agard, D.; Colombo, G.; Bernardi, A. Synthesis of Functionalized 2-(4-Hydroxyphenyl)-3-Methylbenzofuran Allosteric Modulators of Hsp90 Activity. *Eur. J. Org. Chem.* **2016**, *20*, 3349–3364.

(40) Guzzetti, I.; Civera, M.; Vasile, F.; Arosio, D.; Tringali, C.; Piarulli, U.; Gennari, C.; Pignataro, L.; Belvisi, L.; Potenza, D. Insights into the Binding of Cyclic RGD Peptidomimetics to A5 β 1 Integrin by Using Live-Cell NMR And Computational Studies. *ChemistryOpen* **2017**, *6*, 128–136.

(41) Monaco, S.; Tailford, L. E.; Juge, N.; Angulo, J. Differential Epitope Mapping by STD NMR Spectroscopy To Reveal the Nature of Protein–Ligand Contacts. *Angew. Chem., Int. Ed.* **2017**, *56*, 15289–15293.